ADVANCED FUNCTIONAL MATERIALS
www.afm-journal.de

Direct Growth of Nanographene on Silicon with Thin Oxide Layer for High-Performance Nanographene-Oxide-Silicon Diodes

*Qichong Zhang, Xiaojuan Wang, Dong Li, and Zengxing Zhang**

Graphene-silicon based configurations are attracting great attention for their potential application as electronics and optoelectronics. For their practical use, it is still limited by the configuration fabrication process. In this paper, a catalyst-free method is reported to directly grow nanographene on silicon covered with a thin oxide layer to form nanographene-oxide-silicon configurations. Compared with previously reported nanographene-silicon Schottky junctions, the nanographene-oxide-silicon structures exhibit a high performance on electronic and photovoltaic properties. The reverse leakage current of the nanographene-oxide-silicon is suppressed from over 10^{-5} A down to 10^{-8} A and the rectifier ratio is greatly enhanced from less than 5 up to 10^3. The photovoltage is enhanced over 50 times. The nanographene-oxide-silicon structures exhibit especially ultrasensitive to weak light at a photovoltage working mode, which exceeds up to 10^6 V/W at the light power of 0.025 μW. Due to the source material for nanographene is photoresist and the fabrication process is mainly based on the current-used photolithography and silicon technique, the developed nanographene-oxide-silicon structures are very easy for device fabrication, integration, and miniaturization, and could be a promising way to produce metal-free graphene-silicon based electronics and optoelectronics for commercial use.

1. Introduction

Graphene, a single layer of carbon atoms packed with a honeycomb structure, has been attracting tremendous attention owing to its excellent mechanical flexibility, outstanding optical transparency and high-performance electronic properties.[1–6] Theoretical and experimental results indicate that monolayer graphene has a sheet resistance as low as 30 Ω/□ with an absorption of only 2.3% for visible light.[7,8] These remarkable properties make graphene a promising candidate for future stretchable transparent electrodes.[5,9] It is thus stimulating intense studies on the development of high-performance graphene transparent electrodes and their applications for solar cells, light-emitting diodes (LEDs), photodetectors, touch screens, and so on.[5,10–19] Among these studies, the combination of graphene transparent electrodes and silicon for optoelectronics is attracting especial attention concerning that silicon is a widely used commercial material in semiconductor industry. Li et al. found that graphene and silicon can form Schottky junction, and thus developed the configurations for solar cells.[20] Through tuning the configurations, Miao et al. reported that the graphene-silicon (GS) junctions exhibited a power conversion efficiency of 8.6%,[21] and Shi et al. further developed the efficiency up to 14.5%.[22] Moreover, An et al. reported that the GS Schottky junctions can be employed as ultrasensitive photodetectors with a photovoltage responsivity exceeding to 10^7 V/W at a low light power of 10 nW.[19] These excited results are motivating the scientific community to develop GS structures for practical applications.[23–25]

However, it is still a big problem to produce GS configurations for large-scale applications so far. Graphene used in these structures is mainly through mechanical cleavage or chemical vapor deposition (CVD) methods.[19–22,26] The former method is not suitable for large-scale applications, and the later is often with an inevitable transferring procedure leading to the process complicated, cost increasing and environment polluted. Recently, we developed a catalyst-free method to directly grow large-scale nanocrystalline graphene-graphite patterns on various substrates from photoresist,[27] and successfully made them apply for transparent electrodes on silicon to form metal-free GS Schottky diodes, where nanographene serves as transparent electrodes and nanographite serves as leads to connect the nanographene and the outer circuit.[28] Due to that the process is based on the conventional photolithography and silicon technique without any transfer, it gives a possibility to produce practical GS Schottky junctions for future commercial applications. But because of that the process needs high temperature treatment, carbon atoms always diffuse into silicon resulting in defects and complicated surface states in silicon interface, leading to that the produced GS Schottky junctions exhibit a high reverse leakage current and a poor rectifier

Dr. Q. C. Zhang, Dr. X. J. Wang, Dr. D. Li, Prof. Z. X. Zhang
MOE Key Laboratory of Advanced Micro-structured Materials
Shanghai Key Laboratory of Special Artificial Microstructure Materials and Technology
School of Physics Science and Engineering
Tongji University
Shanghai 200092, China
E-mail: zhangzx@tongji.edu.cn

DOI: 10.1002/adfm.201402099

ratio. In comparison with metal-semiconductor Schottky structures, metal-insulator-semiconductor (MIS) structures with a thin insulator layer inserted between the metal and the semiconductor often show a high open-circuit voltage (V_{OC}) and should be a promising structure for high-performance photovoltaic devices. In this paper, we reported a simple approach to directly grow nanographene on silicon for metal-free nanographene-oxide-silicon (GOS) configurations through previously inserting a thin thermal oxide insulator layer between the nanographene and the silicon. The results exhibit that the inserted oxide layer can effectively and greatly suppress the reverse leakage current and strongly enhance the rectifier ratio. The GOS configurations also show much better photovoltaic properties compared with the GS structures produced with a similar method, and are even competitive to the GS devices with CVD-derived graphene. The whole process is mainly based on the conventional photolithography and silicon technique and it thus supplies one practical way to produce high-performance, low-cost and large-scale graphene-silicon based metal-free electronics and optoelectronics.

2. Results and Discussion

Figure 1a–e show a schematic process of the GOS configurations fabrication, and the details can be seen in the experimental section and Figure S2 in Supporting Information. High temperature treatment can transform photoresist film into nanographite with nanographene formed on the clean neighbor part without photoresist due to the carbonization and graphitization.[27,28] Figure 1f shows an optical photograph of a produced typical GOS configuration and its schematic cross section. The GOS configurations are almost similar to our previously reported GS Schottky junctions except that there is a thin thermal oxide layer inserted between the nanographene and the silicon.[28] The thin oxide layer is about 2.5 nm in thickness and 0.5×0.5 mm^2 in area. For devices measurement, the outer circuit is connected with the nanographite on the 300-nm-thick SiO_2 and the underneath silicon. They thus exhibit a metal-free configuration.

Figure 2a and 2b show current–voltage (*I–V)* characteristic curves of a typical GOS configuration and a typical GS configuration under the dark condition. The fabrication details of the GS configurations are shown in the experimental section as reported in our previous results.[28] As shown in the figures, the GS configuration shows a Schottky behavior with a large reverse leakage current at around 10^{-5} A and a poor rectifier ratio. The reverse leakage current keeps on increasing with the bias voltage increasing without any obvious saturation. Typically, this kind of GS configurations has a rectifier ratio less than 5. The current at the zero bias voltage is about 10^{-7} A, which is close to the reported results.[20] However, in comparison of the produced GS configurations, the GOS configurations exhibit a pretty excellent rectifying property. As shown in the figures, the GOS configuration shows a rather low reverse leakage current of about 10^{-8} A, indicating that the reverse leakage current is reduced 10^3 times. Typically, the rectifier ratio of the produced GOS configurations is about 10^3, which is strongly enhanced compared with the GS configurations (less than 5). It should be noted here that the current at the zero bias voltage is also suppressed. For GOS, it is less than 10^{-9} A.

Since there is no difference between the GOS and the GS except for the inserted thin oxide layer, the enhancement of the electronic behaviors of the GOS could be decided to originate from the thin oxide layer. For the GS configurations, the high temperature treatment process (1000 °C) could make carbon atoms diffuse into the silicon near the interface. The diffused carbon atoms result in defects in silicon and would lead to a high interfacial defect density state. The large reverse leakage current of the GS is probably due to the high interfacial defect

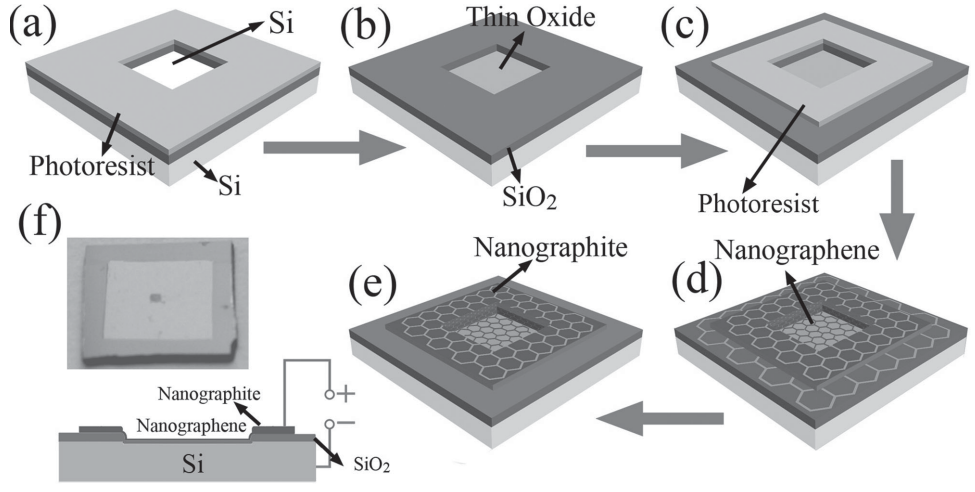

Figure 1. a–e) Schematic fabrication process of the metal-free nanographene-oxide-silicon (GOS) configuration. a) An area of 0.5×0.5 mm^2 SiO_2 is totally etched by BOE with the photoresist protecting. b) After the photoresist is removed, the exposed silicon is oxidized to form a thin oxide layer of ~2.5 nm on. c) A photoresist structure is aligned on the Si/SiO_2 configuration. d) After high-temperature treatment, the photoresist film is transformed into nanographite with nanographene formed on the around parts. e) The nanographene on the around part is etched by oxygen plasma to avoid the possible contact between the nanographene and the side silicon. f) Optical photograph of a produced metal-free nanographene-oxide-silicon device and its schematic cross section view.

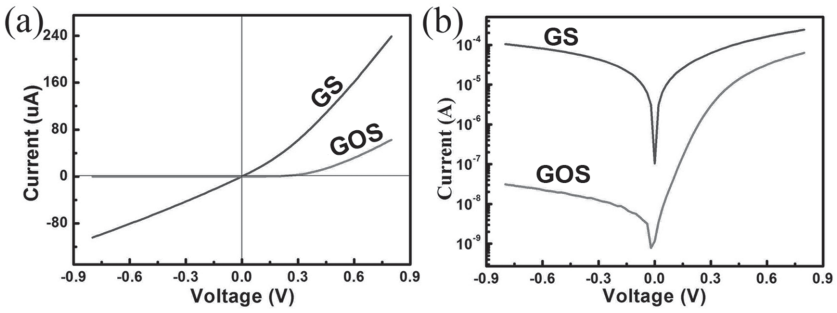

Figure 2. a,b) *I–V* curves of a typical nanographene-oxide-silicon (GOS) device and a typical nanographene-silicon (GS) device in different y axis scale.

density state. In the GOS configurations, the thin oxide layer plays at least two roles. One is as a passivation layer to block the carbon atoms diffusing into the silicon during the high temperature treatment process; the other role should be as an insulator layer between the nanographene and the silicon to make the GOS configurations serve as a metal-insulator-semiconductor (MIS) structure. As what is demonstrated in the experimental section, the inserted thin oxide layer is only about 2.5 nm in thickness. At this situation, the current across the GOS should be dominated by the thermionic emission tunneling limited mode rather than others.[29–34] (The temperature dependent *I–V* characteristic curves of the GOS can be seen in Figure S5 in Supporting Information.) It means that the GOS configurations here serve as a MIS tunneling diode. The thin oxide layer, as a well-known insulator, plays as an effective barrier to make the current across the configurations dominated by a thermionic emission tunneling mode. On the contrary, the barrier in the GS Schottky junction is affected by the high interfacial density state in silicon from the diffused carbon atoms, resulting in that the reverse leakage current is pretty high.

The thin oxide insulator layer in MIS structures often makes the thermionic emission current from the majority carriers decrease, but is nearly no effect on the current from the diffused minority carriers (as shown in **Figure 3**a). It could thus be used to increase the open-circuit voltage (V_{OC}) of the Schottky photovoltaic devices.[29] Therefore, it is possible to use the developed GOS structures for high-performance photodetectors working at a photovoltage mode. Figure 3b shows *I–V* characteristic curves of the GOS under the darkness and the light illumination, respectively. The light source used here is a white light-emitting diodes (LEDs) lamp, the power of which can be continually modulated up to 5.5 mW/cm^2. Obviously, the GOS device exhibits a conventional rectifying behavior and a remarkable photovoltaic property under the light illumination. It means that the incident light can pass through the nanographene transparent electrode and the inserted thin oxide layer, and then generates electron-hole pairs in silicon. The photo-excited carriers are separated by the built-in electric field in the GOS structures, resulting in the holes being transported from the silicon to the nanographene and then to the nanographite around (Figure 3a). By this way, the photovoltage is generated in the GOS structure.

The photovoltaic behavior of the GOS structure varies with the light power varying. As shown in Figure 3c, the V_{OC} and I_{SC} keep on increasing with the light power increasing. This indicates that the GOS can be developed for photodetectors. Photovoltage measurement is a promising mode for sensitive photodetection due to the zero bias current without any Joule-heating associated with energy consumption. We thus tested the GOS at a photovoltage mode. Figure 3d shows the time-dependent photovoltage response of the GOS device to the light with different power switching on and off for six cycles. The results indicate that the photovoltage is generated while the light switches on, and rapidly shuts off while the light switches off. The generated photovoltage obviously increases with the light power increasing. Under the light power of 0.025 μW, the generated photovoltage is about 27 mV; while the light power increases to 10 μW, the photovoltage increases up to ~156 mV.

Compared with the GS Schottky junctions, the GOS devices exhibit much more sensitive to the light. **Figure 4**a shows time-dependent photovoltage response curves of the GOS device and the GS device with the light switching on and off for six cycles.

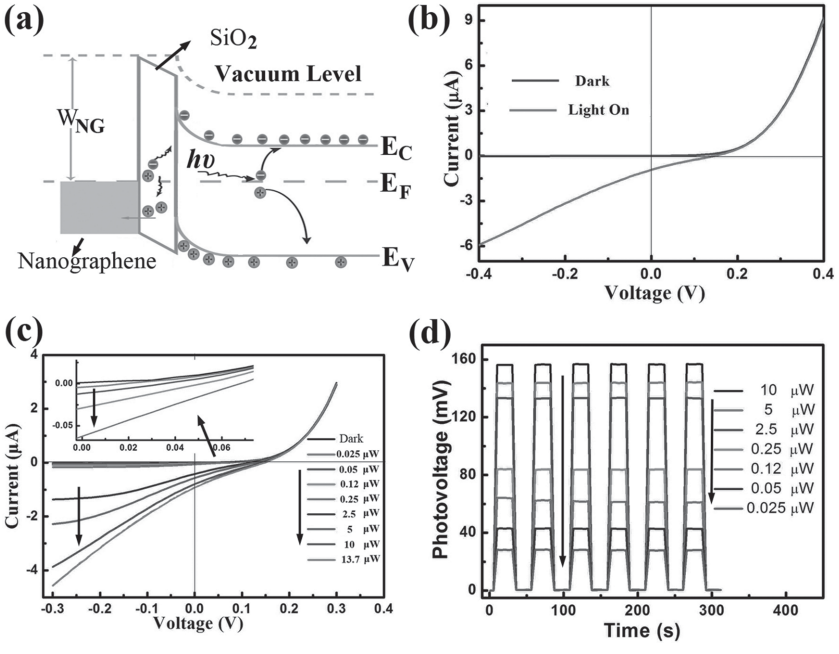

Figure 3. a) Energy diagram of the nanographene-oxide-silicon (GOS) under light illumination. W_{NG} is the working function of the nanographene. b) *I–V* curves of the GOS under the dark and the light illumination. The light power is ca.13.7 μW. c) *I–V* curves of the GOS under the dark and the light illumination with different power. d) Photovoltage (V_{OC}) response of the GOS to the light with different power switching on and off.

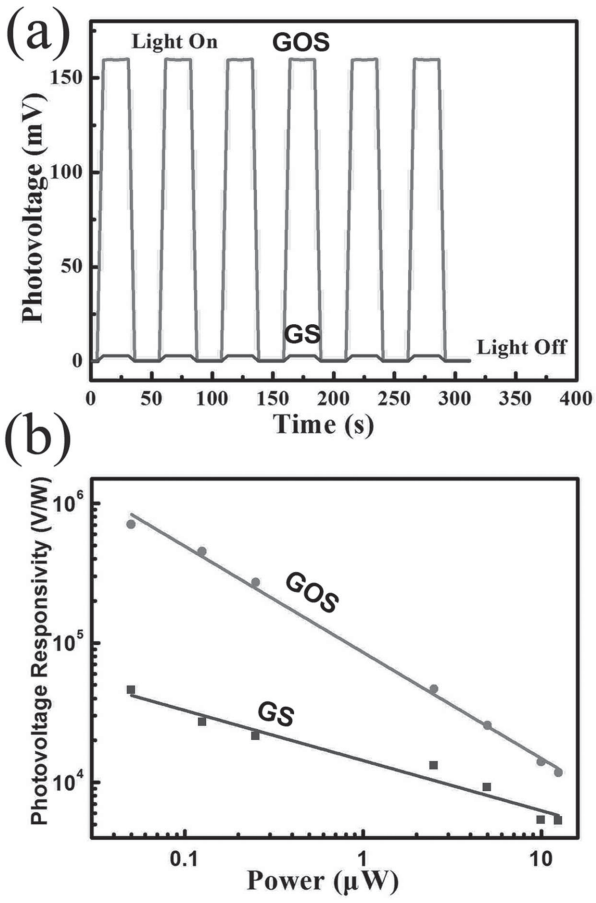

Figure 4. a) Photovoltage (V_{OC}) response of the GOS device and the GS device to the light switching on and off. The light power is ~13.7 μW. b) Photovoltage (V_{OC}) responsivity of the GOS device and the GS device with different light power. The responsivity is defined as V_{OC}/P, P is the incident light power.

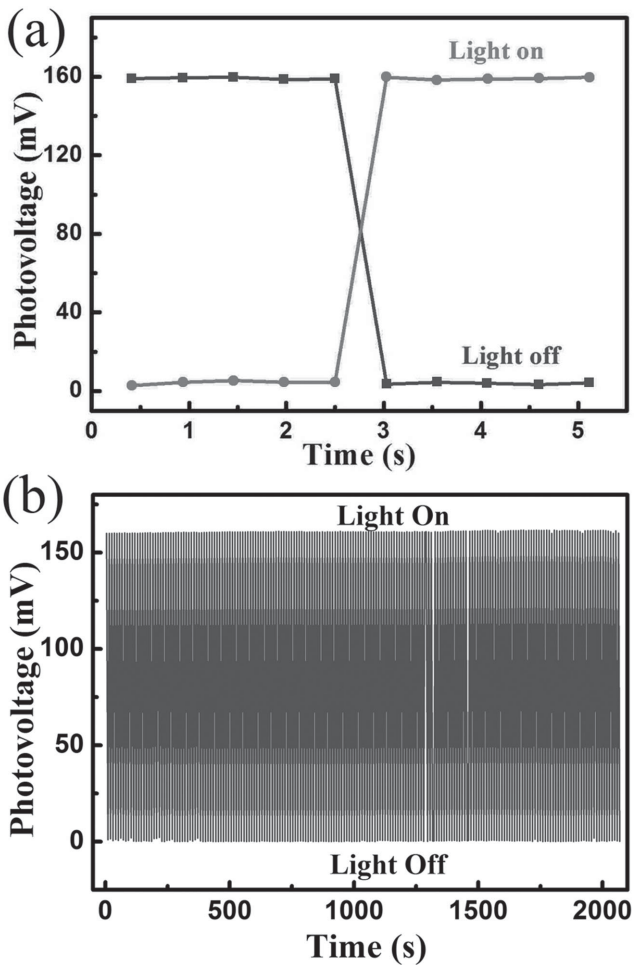

Figure 5. a) Photovoltage (V_{OC}) response of the GOS device to the light switching on and off. b) Time-dependent repeatability of switching properties of the GOS device for over 200 times. The light power is ca.13.7 μW.

Both of them are tested under the light power of ~13.7 μW. The results clearly indicate that the GOS generates a much higher photovoltage than the GS. Under the light illumination, the GS structure shows a photovoltage of about 3 mV, while the GOS structure exhibits a high photovoltage up to 160 mV. It increases over 50 times. Figure 4b shows the responsivity of the GOS and the GS to the light with different power. The responsivity R_S is defined as V_{OC}/P; P is the incident light power. The results exhibit that both of them are almost linearly increase with the light power decreasing, which is similar to the reported results.[19,28] However, the GOS shows an obviously higher responsivity than the GS. And with the light power decreasing, the responsivity of the GOS increases much faster. At the light power of 10 μW, the responsivity of the GOS is about 10^4 V/W; while the light power decreases to 0.025 μW, the responsivity increases up to 10^6 V/W, indicating that the GOS should be especially suitable for ultrasensitive photodetectors to weak light. In fact, the responsivity of the GOS structure is even competitive to the GS Schottky junctions produced with CVD-derived graphene.[19] But the producing process is much easier and of low cost, indicating it should be competitive for the future graphene-silicon based optoelectronic devices.

Response time is an important characteristic for photodetectors. The photodetectors with a fast response time indicate that they can switch quickly from "on" to "off" state or from "off" to "on" state along with the light. **Figure 5**a shows the photovoltage response time of the GOS to the light switching on and off. The power of the light is 13.7 μW. Unfortunately, we can not exactly obtain the real response time of the GOS to the light due to the equipment limitation. The rough measurements clearly indicate that the response time is less than 0.5 s. For practical applications, reliability should be considered seriously. Figure 5b shows the photovoltage response curve of the GOS to the light cycling on and off for over 200 times. The results show that the deviated photovoltage is less than 0.5%, indicating that the GOS device has an excellent repeatability.

3. Conclusions

We thus developed a simple and low cost method to produce metal-free nanographene-oxide-silicon (GOS) configurations. Compared with the nanographene-silicon (GS) Schottky structures produced with the similar method, the GOS structures

exhibit high performances on electronic and photovoltaic properties. Due to the thin oxide layer inserted, the reverse leakage current of the GOS is effectively suppressed from over 10^{-5} A down to 10^{-8} A and the rectifier ratio is greatly enhanced from less than 5 up to 10^3. The photovoltaic properties are also enhanced due to the GOS can suppress the thermionic emission current from the major carriers and has nearly no effect on the minor carriers diffusion. The open-circuit voltage (V_{OC}) of the GOS is increased from ~3 mV up to ~160 mV in comparison of the GS structure under the light illumination with the power of 13.7 μW. The GOS structures exhibit especially ultrasensitive to weak light. Under the light power of 0.025 μW, the responsivity of the GOS exceeds up to 10^6 V/W, which is much better than the GS structures produced with the similar method and even competitive to the GS structures with CVD-derived graphene. Due to the source material for the nanographene here is photoresist and the GOS produced in this way is mainly based on the current-used photolithography and silicon technique, the GOS configurations are very easy to achieve device fabrication, integration, and miniaturization; it could thus be a practical way to produce metal-free graphene-silicon based electronics and optoelectronics for commercial use.

4. Experimental Section

Materials: The silicon wafer used in the experiment is *n*-type with a resistivity of 1–10 Ω·cm, covered with a 300-nm-thick thermal oxide film. The photoresist is RZJ-304 from Suzhou Ruihong Electronic Chemicals Co. Ltd. It is a positive photoresist.

Fabrication of Metal-Free Nanographene-Silicon (GS) Schottky Diodes: Metal-free GS Schottky diodes were fabricated as what we reported previously (schematically demonstrated in Figure S1 in Supporting Information).[28] Firstly, 1.5-μm-thick photoresist film was spin-coated on the Si/SiO_2 wafer and a square window with an area of 0.5×0.5 mm^2 was cleaned with a standard photolithography method. The exposed SiO_2 layer in the window was then totally wet-etched by buffered oxide etchant (BOE, NH_4F : 10% HF : H_2O = 8 g : 2 ml : 12 ml) leading to the underneath silicon present. In order to avoid the contact between the photoresist and the side silicon, the around photoresist was also totally etched by photolithography. The obtained structures were then heated for 10 minutes in a vacuum horizontal quartz tube at 1000 °C under the protection of 100 SCCM 5% H_2/Ar gas flow. The photoresist structure thus in situ grew into nanographite with nanographene formed on the surface of the part (including the exposed silicon) without photoresist. Finally, the nanographene on the surface of the around part was etched by oxygen plasma to avoid the possible contact between the nanographene and the side silicon. It should be noted here that the origination of the nanographite growth is due to the high-temperature carbonization and graphitization. The formation of the nanographene around the photoresist structure originates from the photoresist molecules evaporation and transportation.[27,28] After these procedures, metal-free GS Schottky diodes were ready for characterization where nanographite served as electrodes instead of metal.

Fabrication of Metal-Free Nanographene-Oxide-Silicon (GOS) Diodes: Metal-free GOS comfigurations were fabricated as following (demonstrated in Figure 1a–e and Figure S2 in Supporting Information): (1) 1.5-μm-thick photoresist film was spin-coated on the Si/SiO_2 wafer and a square window with an area of 0.5×0.5 mm^2 was cleaned with a standard photolithography method. (2) The exposed SiO_2 layer in the window was totally wet-etched by BOE leading to the underneath silicon present. (3) The photoresist film on the Si/SiO_2 structure was carefully cleaned by acetone and DI water in sequence. The Si/SiO_2 structure was then dried by N_2 gas flow. (4) The dried Si/SiO_2 structure was treated in air gas flow at 800 °C for 30 minutes to get a 2.5-nm-thick thermal oxide film on the exposed silicon window. The determining method of the thickness of the thermal oxide film can be seen in Figure S3 in Supporting Information. (5) 1.5-μm-thick photoresist structure was aligned on the square window. (6) The obtained structure was heated for 10 minutes in a vacuum horizontal quartz tube at 1000 °C under the protection of 100 SCCM 5% H_2/Ar gas flow. Photoresist structure grew into nanographite with nanographene formed on the surface of the part (including the window) without photoresist. (7) Nanographene on the around part was etched by oxygen plasma to avoid the possible contact between the nanographene and the side silicon. After the above procedures, metal-free GOS diodes were ready for characterization, where nanographite served as electrodes instead of metal.

Characterizations: The thickness of the thermal oxide film was decided by atomic force microscopy (AFM). The nanographene was characterized by Raman spectroscopy. The electrical and photoelectrical properties of the produced diodes were characterized with a Keithley 4200-SCS semiconductor analyzer at room-temperature in atmosphere. The light source was a light-emitting diode (LED) lamp whose power can be modulated. We used an optical power meter of SGN-1 to measure the power of the light and calculated the incident light power on the configurations according to their area.

Supporting Information

Supporting Information is available from the Wiley Online Library or from the author.

Acknowledgements

The work was supported by NSFC (11104204) and Shanghai Pujiang Program (12PJ1408900). The authors thank Dr. Liping Zou for Raman spectroscopy measurement.

Received: June 25, 2014
Revised: September 1, 2014
Published online: September 30, 2014

[1] A. K. Geim, K. S. Novoselov, *Nat. Mater.* **2007**, *6*, 183.
[2] Y. Zhang, Y.-W. Tan, H. L. Stormer, P. Kim, *Nature* **2005**, *438*, 201.
[3] C. Lee, X. Wei, J. W. Kysar, J. Hone, *Science* **2008**, *321*, 385.
[4] A. H. Castro Neto, F. Guinea, N. M. R. Peres, K. S. Novoselov, A. K. Geim, *Rev. Mod. Phys.* **2009**, *81*, 109.
[5] K. S. Novoselov, V. I. Falko, L. Colombo, P. R. Gellert, M. G. Schwab, K. Kim, *Nature* **2012**, *490*, 192.
[6] H. Zhou, C. Qiu, Z. Liu, H. Yang, L. Hu, J. Liu, H. Yang, C. Gu, L. Sun, *J. Am. Chem. Soc.* **2009**, *132*, 944.
[7] J.-H. Chen, C. Jang, S. Xiao, M. Ishigami, M. S. Fuhrer, *Nat. Nano.* **2008**, *3*, 206.
[8] R. R. Nair, P. Blake, A. N. Grigorenko, K. S. Novoselov, T. J. Booth, T. Stauber, N. M. R. Peres, A. K. Geim, *Science* **2008**, *320*, 1308.
[9] K. S. Kim, Y. Zhao, H. Jang, S. Y. Lee, J. M. Kim, K. S. Kim, J.-H. Ahn, P. Kim, J.-Y. Choi, B. H. Hong, *Nature* **2009**, *457*, 706.
[10] H. Medina, Y.-C. Lin, C. Jin, C.-C. Lu, C.-H. Yeh, K.-P. Huang, K. Suenaga, J. Robertson, P.-W. Chiu, *Adv. Func. Mater.* **2012**, *22*, 2123.
[11] Y. Zhu, Z. Sun, Z. Yan, Z. Jin, J. M. Tour, *ACS Nano* **2011**, *5*, 6472.
[12] X. Li, Y. Zhu, W. Cai, M. Borysiak, B. Han, D. Chen, R. D. Piner, L. Colombo, R. S. Ruoff, *Nano Lett.* **2009**, *9*, 4359.
[13] X. Wang, L. Zhi, K. Mullen, *Nano Lett.* **2007**, *8*, 323.
[14] H. Chang, H. Wu, *Adv. Func. Mater.* **2013**, *23*, 1984.
[15] V. C. Tung, L.-M. Chen, M. J. Allen, J. K. Wassei, K. Nelson, R. B. Kaner, Y. Yang, *Nano Lett.* **2009**, *9*, 1949.

[16] S. Bae, H. Kim, Y. Lee, X. Xu, J.-S. Park, Y. Zheng, J. Balakrishnan, T. Lei, H. Ri Kim, Y. I. Song, Y.-J. Kim, K. S. Kim, B. Ozyilmaz, J.-H. Ahn, B. H. Hong, S. Iijima, *Nat. Nano.* **2010**, *5*, 574.
[17] Z. Liu, Q. Liu, Y. Huang, Y. Ma, S. Yin, X. Zhang, W. Sun, Y. Chen, *Adv. Mater.* **2008**, *20*, 3924.
[18] T. H. Han, Y. Lee, M. R. Choi, S. H. Woo, S. H. Bae, B. H. Hong, J. H. Ahn, T. W. Lee, *Nat. Photonics* **2012**, *6*, 105.
[19] X. An, F. Liu, Y. J. Jung, S. Kar, *Nano Lett.* **2013**, *13*, 909.
[20] X. Li, H. Zhu, K. Wang, A. Cao, J. Wei, C. Li, Y. Jia, Z. Li, X. Li, D. Wu, *Adv. Mater.* **2010**, *22*, 2743.
[21] X. Miao, S. Tongay, M. K. Petterson, K. Berke, A. G. Rinzler, B. R. Appleton, A. F. Hebard, *Nano Lett.* **2012**, *12*, 2745.
[22] E. Shi, H. Li, L. Yang, L. Zhang, Z. Li, P. Li, Y. Shang, S. Wu, X. Li, J. Wei, K. Wang, H. Zhu, D. Wu, Y. Fang, A. Cao, *Nano Lett.* **2013**, *13*, 1776.
[23] C. Xie, P. Lv, B. Nie, J. Jie, X. Zhang, Z. Wang, P. Jiang, Z. Hu, L. Luo, Z. Zhu, L. Wang, C. Wu, *Appl. Phys. Lett.* **2011**, *99*, 133113.
[24] M. Zhu, X. M. Li, Y. B. Guo, X. Li, P. Z. Sun, X. B. Zang, K. L. Wang, M. L. Zhong, D. H. Wu, H. W. Zhu, *Nanoscale* **2014**, *6*, 4909.
[25] X. M. Wang, Z. Z. Cheng, K. Xu, H. K. Tsang, J. B. Xu, *Nat. Photonics* **2013**, *7*, 888.
[26] C.-C. Chen, M. Aykol, C.-C. Chang, A. F. J. Levi, S. B. Cronin, *Nano Lett.* **2011**, *11*, 1863.
[27] Z. X. Zhang, B. H. Ge, Y. Guo, D. Tang, X. Wang, F. Wang, *Chem. Commun.* **2013**, *49*, 2789.
[28] Z. X. Zhang, Y. Guo, X. Wang, D. Li, F. Wang, S. S. Xie, *Adv. Func. Mater.* **2014**, *24*, 835.
[29] S. M. Sze, K. K. Ng, *Physics of Semiconductor Physics*, Third Edition, Wiley, New York, USA **2006**, Ch. 3.3.6.
[30] K. C. Kao, W. Hwang, *Electrical Transport in Solids*, Pergamon, New York, USA **1981**, Chs. 2, 3, 5.
[31] H.-J. Chung, J. H. Jeong, T. K. Ahn, H. J. Lee, M. Kim, K. Jun, J.-S. Park, J. K. Jeong, Y.-G. Mo, H. D. Kim, *Electrochem. Solid-State Lett.* **2008**, *11*, H51.
[32] C. S. Hwang, *J. Mater. Res.* **2001**, *16*, 3476.
[33] F. D. Morrison, P. Zubko, D. J. Jung, J. F. Scott, P. Baxter, M. M. Saad, R. M. Bowman, J. M. Gregg, *Appl. Phys. Lett.* **2005**, *86*, 152903.
[34] J. G. Simmons, *Phys. Rev. Lett.* **1965**, *15*, 967.